International Journal of Chemical Science
Online ISSN: 2523-2843, Print ISSN: 2523-6075
Impact Factor: RJIF 5.22
www.chemicaljournals.com
Volume 2; Issue 5; September 2018; Page No. 22-27

Influence of Cu substitution on structural properties of $Ni_{0.7}Co_{0.3-x}Cu_xFe_2O_4$ ferrites

G Satyanarayana[1], G Nageswara Rao[2*], K Vijaya Babu[3]
[1, 2] School of Chemistry, Andhra University, Visakhapatnam, Andhra Pradesh, India
[1, 3] Advanced Analytical Laboratory, Andhra University, Visakhapatnam, Andhra Pradesh, India

Abstract
Copper substituted Ni0.7Co0.3-xCuxFe2O4 (x=0.0, 0.05, 0.1, 0.15 and 0.2) nanocrystalline ferrites are synthesized by the sol-gel method. The x-ray powder diffraction (XRD) patterns show that all samples have a pure single-phase cubic spinel structure with Fd-3m space group over the whole composition range. From XRD patterns, the lattice constants, average crystallite size, grain size of these compounds have also been calculated and compared to nickel ferrite. Most of the values are found to be increased with increasing copper concentration.

Keywords: spinel ferrite, XRD, SEM-EDS, FTIR

Introduction
The ferrites are magnetic ceramics consisting of iron oxide and metal oxides finds potential applications for making many devices such as permanent magnets, memory storage devices, microwave devices and telecommunication equipment. The high electrical resistivity, low dielectric loss, high saturation magnetization, high permeability, moderate permittivity etc. are the remarkable electrical and magnetic features of ferrites [1-3]. Spinel ferrites are made up of a regular combination of oxygen with the general formula of AB_2O_4. The unit cell of spinel ferrites is composed of 32 oxygen atoms in cubic closed packed arrangement distributed in tetrahedral (A) and octahedral sites (B) [4-6]. Chemical and structural properties of spinel nanocrystalline ferrite are highly sensitive to their compositions and synthesis methods, and corresponding electric and magnetic properties depends on cation substitutions. Among the spinel ferrites, the inverse type is more interesting due to its high magneto crystalline anisotropy and high saturation magnetization [7-8]. Nickel ferrite ($NiFe_2O_4$) is one of the most important materials in the inverse spinel family exhibiting magnetic properties combined with electrical properties. Also, the substituted nickel ferrite has been widely studied due to their typical properties, high saturation magnetization, low conductivity, low dielectric losses and low cost etc. making a good candidate for the application as soft magnets and low loss materials at high frequencies [9-10].
The aim of the present work is to prepare and characterize spinel nanocrystalline ferrites with general formula $Ni_{0.7}Co_{0.3-x}Cu_xFe_2O_4$ (x=0.0, 0.05, 0.1, 0.15 and 0.2) by substituting Cu^{2+} and Co^{2+} in $NiFe_2O_4$. The effects of the substitutions on structural, electrical and magnetic properties are also investigated. The materials are obtained by sol-gel method using citric acid as chelating and fuel agent.

Synthesis and experimental techniques
The $Ni_{0.7}Co_{0.3-x}Cu_xFe_2O_4$ (x=0, 0.05, 0.1, 0.15 and 0.2) nanocrystalline ferrites are synthesized by using sol-gel method. AR chemicals such as nickel nitrate ($Ni(NO_3)_2.6H_2O$), cobalt nitrate ($Co(NO_3)_2.6H_2O$), ferric nitrate ($Fe(NO_3)_3.9H_2O$), copper nitrate $Cu(NO_3)_2.3H_2O$ and citric acid ($C_6H_8O_7$) are used for the synthesis process. The molar metal nitrates to citric acid ratio are taken as 1:3. Ammonia solution is added to maintain the pH-7. The collected compounds are then dried in oven for 2 hours. The powder samples added with polyvinyl alcohol (PVA) as a binder are ground and then pressed at 5 tons / 6 minutes pressure into a circular disk shaped pellet. The synthesized powder and pellet is sintered at 1200 °C for 5 hours and then used for further investigations of structural, morphological, magnetic and electrical properties. The surface layers of the sintered pellet are carefully polished and washed in acetone and then the pellet is coated with silver paste on the opposite faces which act as electrodes.
The synthesized nanocrystalline $Ni_{0.7}Co_{0.3-x}Cu_xFe_2O_4$ (x=0.0, 0.05, 0.1, 0.15 and 0.2) ferrites are characterized by standard techniques such as X-ray powder diffraction (XRD), scanning electron microscope (SEM), electron spin resonance (ESR) and LCR meter. The XRD patterns are recorded at room temperature in the 2θ range of 10° to 70° using Cu-Kα radiation (λ=1.5405Å). The particle morphology of the powders is observed using scanning electron microscopy images taken from JEOL JSM-6610L. Fourier transform infrared (FT-IR) spectra measurements are accomplished by Shimadzu Shimadzu IR-Prestige21 instrument in transmittance method with potassium Bromide (KBr) as IR window in the wave number region of 400 to 1300 cm^{-1}.

Results and discussion
Structural properties
The XRD patterns of nanocrystalline $Ni_{0.7}Co_{0.3-x}Cu_xFe_2O_4$ (x=0.0, 0.05, 0.1, 0.15 and 0.2) ferrites are shown in figure 1.

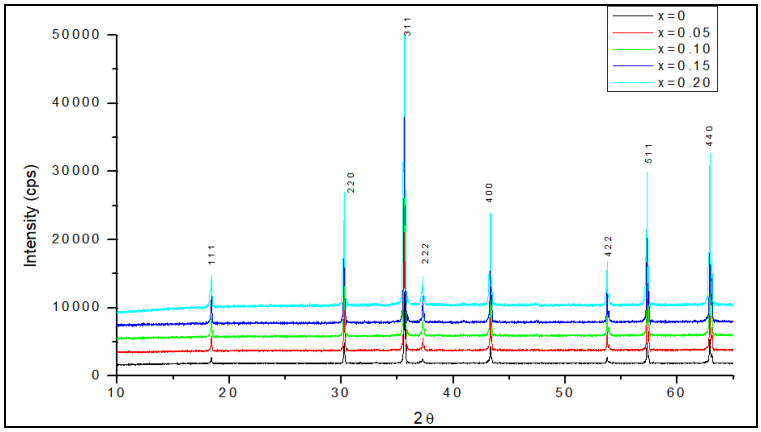

Fig 1: XRD patterns of $Ni_{0.7}Co_{0.3-x}Cu_xFe_2O_4$ (x=0.0, 0.05, 0.1, 0.15 and 0.2)

The XRD patterns are found to be sharp and intense. The patterns are well matched with the characteristic reflections of FCC single phase spinel structure with Fd-3m space group and without identified extra peaks. All the compounds exhibited the maximum intensity at (311) and the presence of the strong diffraction peaks corresponding to the planes (111), (220), (311), (222), (422), (511), (440) and (533) indexed *hkl* values and labelled. The interplanar spacing values for all the compounds are listed in table 1.

Table 1: Inter planer spacing (d) of $Ni_{0.7}Co_{0.3-x}Cu_xFe_2O_4$ (x=0.0, 0.05, 0.1, 0.15 and 0.2)

Plane *h k l*	Interplanar distance (Å)				
	***x*=0**	***x*=0.05**	***x*=0.10**	***x*=0.15**	***x*=2.0**
1 1 1	4.8172	4.8161	4.8185	4.8143	4.8126
2 2 0	2.9512	2.9505	2.9513	2.9498	2.9631
3 1 1	2.5171	2.5168	2.5172	2.5160	2.5262
2 2 2	2.4097	2.4096	2.4102	2.4094	2.4178
4 2 2	2.0872	2.0872	2.0874	2.0867	2.0933
5 1 1	1.7044	1.7045	1.7048	1.7042	1.7081
4 4 0	1.6070	1.6072	1.6072	1.6068	1.6063
5 3 3	1.4762	1.4726	1.4725	1.4718	1.4751

Figure 2: clearly shows the continuous shift in 2θ with increasing copper concentration and the angle shifts towards higher values. This shift is attributed to increase in lattice parameter [11-13]. The lattice constant (a) of all the samples are calculated by using standard relation $a = d\sqrt{h^2 + k^2 + l^2}$, here d is interplaner spacing and (hkl) are Miller indices. The results obtained from unit cell software and above relation are same are given in table 2.

Table 2: Lattice constant, cell volume, X-ray density, bulk density, porosity and crystallite size of $Ni_{0.7}Co_{0.3-x}Cu_xFe_2O_4$ (x=0.0, 0.05, 0.1, 0.15 and 0.2) nanocrystalline ferrites

x-value	Lattice constant (Å)	Volume $(Å)^3$	x-ray density $(g.cm^{-3})$	Crystallite size (nm)
0	8.3442	580.99	5.3612	12.6115
0.05	8.3444	581.012	5.3659	17.7247
0.10	8.3447	581.085	5.3705	10.9239
0.15	8.3485	581.888	5.3683	10.9451
0.20	8.3693	586.237	5.3337	12.5846

The lattice constant (a) values lies in the range 8.3442 to 8.3693Å and agree with previous studies of spinel ferrites.

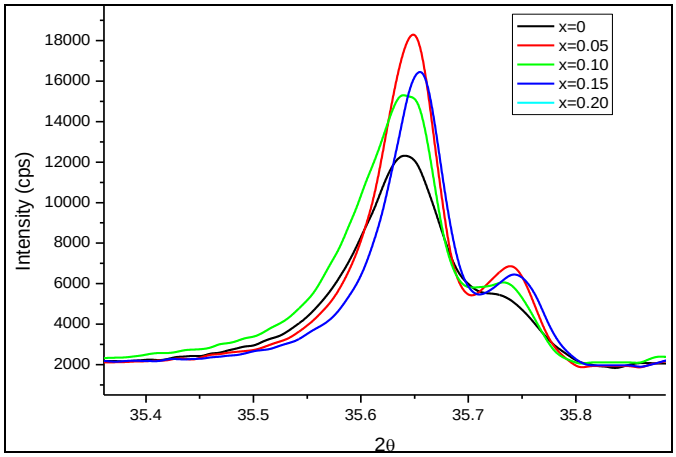

Fig 2: Enlarged view of 311 peak for $Ni_{0.7}Co_{0.3-x}Cu_xFe_2O_4$ (x=0.0, 0.05, 0.1, 0.15 and 0.2)

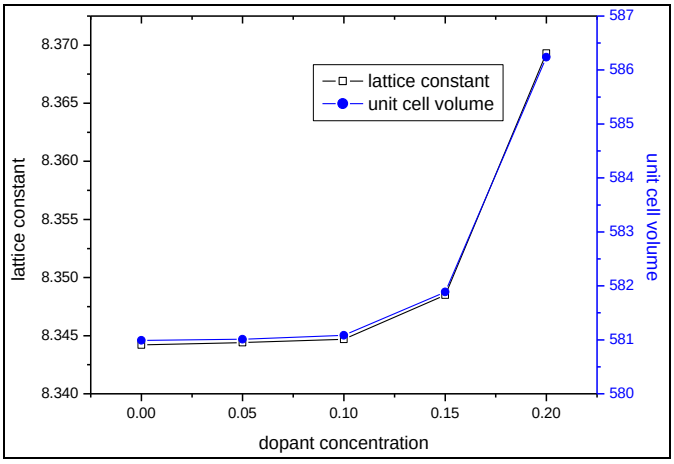

Fig 3: Variation of lattice constant and unit cell volume with dopant concentration

The lattice constant values against the dopant concentration are shown in figure 3. It is seen that the trend of lattice constant is increases slowly with dopant concentration in spite of the substitution of the copper ions instead of the cobalt ions

thereby obeying the Vegard's law [14-16]. The increase in lattice constant is attributed to the difference in the ionic radii of Co^{2+} and Cu^{2+}. The slight variation may be due to slight difference in the ionic radii of Co^{2+} (0.745Å) and Cu^{2+} (0.73Å) ions. The increase in the lattice constant may be due to migration of proportional amount of the large cobalt ion on octahedral (B) site leading to relative expansion of B-site sub lattice, i.e increasing lattice constant. The change of lattice parameters also indicates the change of cation distribution [17-19]. The average crystallite size of the synthesized ferrites has been calculated using the following Debye-Scherer's formula:

$$D = \frac{k\lambda}{\beta \cos\theta}$$

Where *k* is a constant and it depends on the shape of the particle, λ is the x-ray wavelength, β is the full width at half maximum of the most intense peak (311) and θ is the diffraction angle of the peak. The average crystallite size is 10.92 to 12.61nm for different values of dopant concentration. This can be explained in terms of increased pore mobility due to the creation of excess cation vacancies.

Scanning electron microscope

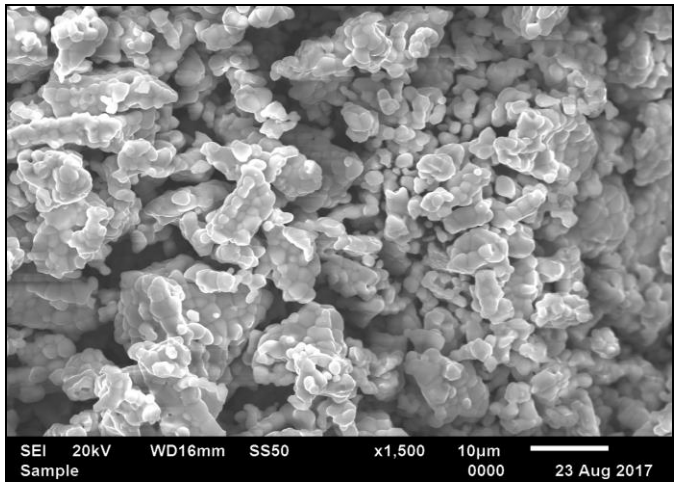

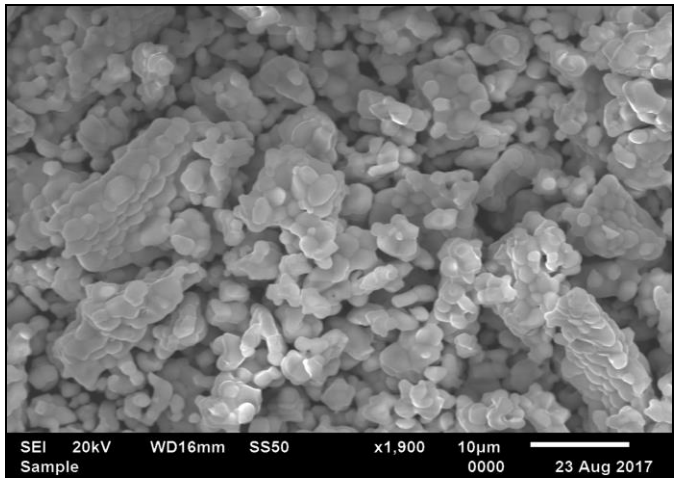

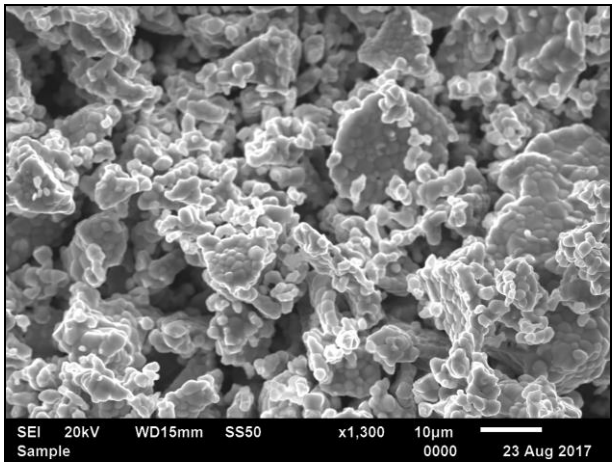

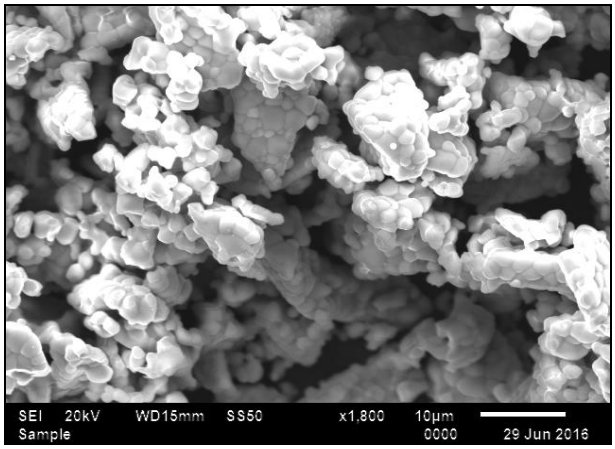

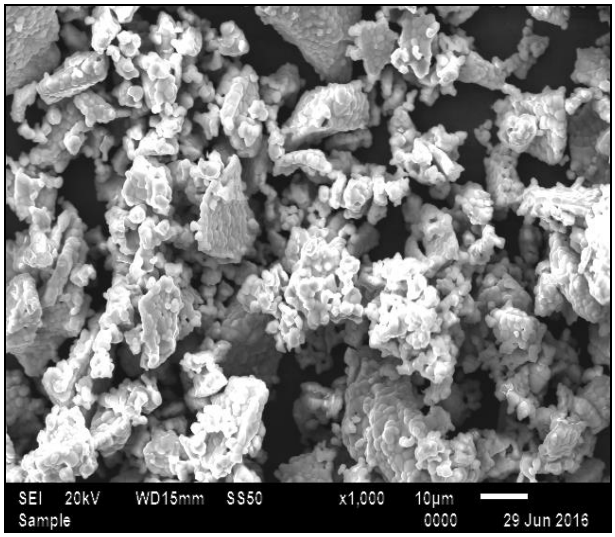

Fig 4: Scanning electron microscopy images of $Ni_{0.7}Co_{0.3-x}Cu_xFe_2O_4$ (*x*=0.0, 0.05, 0.1, 0.15 and 0.2) nano-crystalline ferrites

From the figure 4, observed that the particles are similarly spherical and show the decreasing trend with increasing copper concentration. The average grain size is approximately 10 µm and it is slightly larger than the average crystallite sizes determined by XRD. This is due to that every particle is formed by a number of crystallites or grains. There is a direct

connection between the XRD crystallite size and grain size of the SEM, meaning that a particle can be formed by agglomeration of crystallites. SEM images of $Ni_{0.7}Co_{0.3-x}Cu_xFe_2O_4$ (x=0.0, 0.05, 0.1, 0.15 and 0.2) nanocrystalline ferrites are shown in figures 4. From these figures, it can be seen that the grain size and shape are varying with the dopant concentration significantly. Also, the intergranular pores are not present on the surface of the grains.

EDS and image mapping

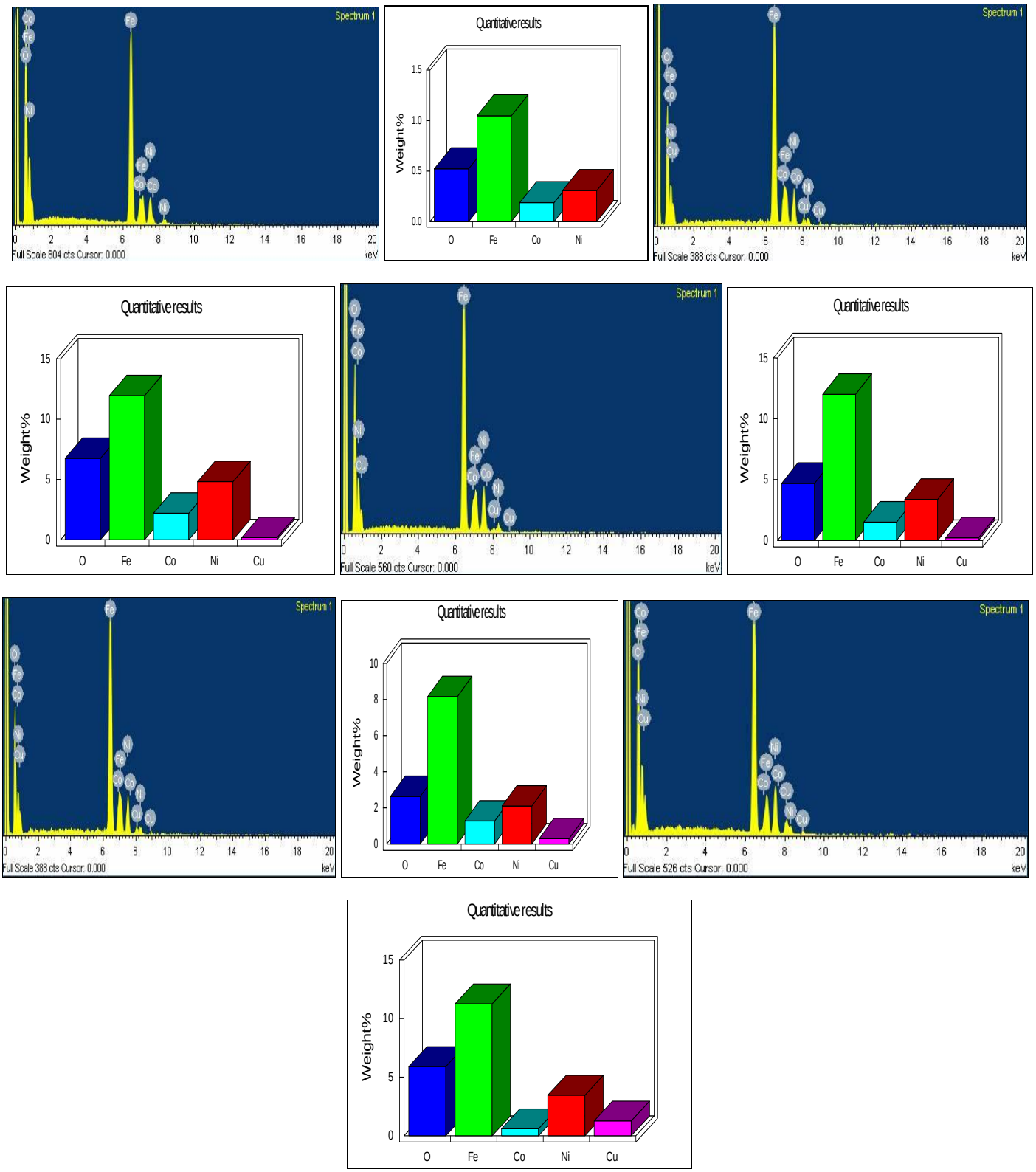

Fig 5: EDS map analysis of $Ni_{0.7}Co_{0.3-x}Cu_xFe_2O_4$ (x=0.0, 0.05, 0.1, 0.15 and 0.2) nano-crystalline ferrites.

The elemental analysis of the samples is obtained from ED's technique using scanning electron microscope. To realize the existence of substituted cations, EDS analysis is carried out on the synthesized ferrites are shown in figures 5 The EDS analysis confirmed the presence of all the elements i.e., Ni, Fe, Co, Cu and O ions in the synthesised samples. Based on the accuracy of EDS, it is clearly observed that no trace of impurity elements is found in the nanocrystalline ferrites. It is confirmed that the final composition of the sample is the same as that of starting composition without any impurity elements. The almost uniform cation concentration distribution is clearly observed throughout the micrographs. The chemical composition of the sample is found to be as per the expectation. It must be mentioned that EDS is a semi-quantitative analysis and the exact amount of cations could not be detected, however it is a rather suitable consistence between the atomic percentage of Ni, Fe, Co, Cu and O in synthesized nanoparticles. By introducing copper in chemical composition of nickel ferrite, the corresponding micrographs are appeared in figure 5. It was found that with an increase in substitution content, the intensity of copper related peaks is enhanced. In the whole series of synthesized nanoparticles, the consistence between the obtained results from EDS and expected chemical composition is suitable [20-21].

Infrared spectra

The FTIR spectra provide the information about the positions taken by ions in the crystal and cation distribution in spinel structure. The FTIR spectra for $Ni_{0.7}Co_{0.3-x}Cu_xFe_2O_4$ (x=0.0, 0.05, 0.1, 0.15 and 0.2) nanocrystalline ferrites in the wave number range 1300-400 cm^{-1} are shown in figure 6. The spectra reveal that the presence of two main absorption peaks at ν_1 and ν_2 wavenumber, which is the characteristic of spinel structure for all samples.

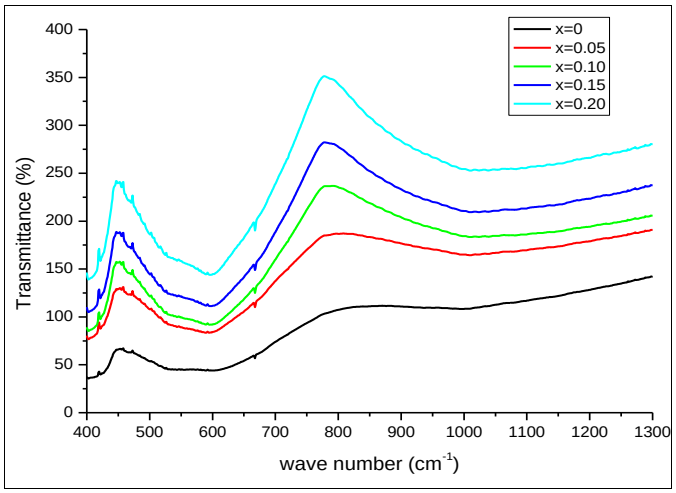

Fig 6: FTIR spectra of $Ni_{0.7}Co_{0.3-x}Cu_xFe_2O_4$ (x=0.0, 0.05, 0.1, 0.15 and 0.2)

The starching bands (ν_2) at higher wave number show the vibration of octahedral site and bands at lower wave number show the vibration of tetrahedral site. The higher frequency band ν_1 is at 667.39 cm^{-1} and the lower frequency band ν_2 is at 419.53cm^{-1}. The difference in the band position is expected because of the difference in the interionic distance for the octahedral and tetrahedral coordinates. A slight shifting of ν_1 bands toward low frequency is expected, because an increase in site radius reduces the fundamental frequency and therefore, the centre frequency of bands should shift toward lower frequency side and vice versa. The vibrational frequency depends on the cation mass, cation to oxygen distance and bonding force. Similar FTIR spectra are also observed in the copper substituted nanocrystalline ferrites. The position of bands in FTIR spectra of all synthesised materials confirmed the formation of spinel ferrite structure.

Conclusion

The nanocrystalline ferrites $Ni_{0.7}Co_{0.3-x}Cu_xFe_2O_4$ (x=0.0, 0.05, 0.1, 0.15 and 0.2) are successfully prepared by sol-gel method using citric acid as fuel and AR grade metal nitrates. The structural, magnetic, electric and dielectric properties of the synthesized ferrites have been studied. The patterns are well matched with the characteristic reflections of FCC single phase spinel structure with Fd3m space group and without identified extra peaks. The lattice constant determined from XRD data increases with increase in copper concentration which is understood from the difference in ionic radii of Co^{2+} and Cu^{2+}. The cation distribution is studied on the basis of intensity ratio calculations. The FTIR spectra illustrate the presence of two absorption bands located near 400 cm^{-1} and 600 cm^{-1} which is the characteristics of a spinel ferrite. The grain size determined by scanning electron microscopy is of the order of 2-4μm. The EDS data suggests that all the elements present in the synthesised ferrites have maintained their stoichiometry properties.

References

1. Sorescu M, Diamandescu L, Peelamedu R, Roy R, Yadoji P. Structural and magnetic properties of NiZn ferrites prepared by microwave sintering, Journal of Magnetism and Magnetic Materials. 2004; 279:195.
2. Upadhyay C, Verma HC, Anand S. Cation distribution in nanosized Ni-Zn Ferrite. Journal of Applied Physics. 2004; 95:5746.
3. Patange SM, Sagar ES, Jangam GS, Lohar KS, Santosh Jadhav S, Jadhav KM. Rietveld structure refinement, cation distribution and magneticproperties of Al^{3+} substituted $NiFe_2O_4$ nanoparticles, Journal of Applied Physics. 2011; 109:053909.
4. SonalSinghal, Kailash Chandra. Cation distribution and magnetic properties in chromium substituted nickel ferrites prepared using aerosol route, J Solid State Chem. 2007; 180:296.
5. Adrian I, Borhan VasileHulea Alexandra R, Iordan Mircea N. $Cr^{3+}$and Al^{3+}co- substituted zinc ferrite: Structural analysis, magnetic and electrical properties", Polyhedron. 2014; 70:110.
6. Zhang HE, Zhang BF, Wang GF, Dong XH, Gao Y. The structure and magnetic properties of $Zn_{1-x}Ni_xFe_2O_4$ ferrite nanoparticles prepared by sol-gel auto-combustion, Journal of Magnetism and Magnetic Materials. 2007; 312:126.
7. Shinde TJ, Gadkari AB, Vasambekar PN. Magnetic properties and cation distribution study of nanocrystalline Ni-Zn ferrites, Journal of Magnetism and Magnetic Materials. 2013; 333:152.

8. Birgani AN, Niyaifar M, Hasanpour A. study of cation distribution of spinel zinc nano-ferrite by X-ray, Journal of Magnetism and Magnetic Materials. 2015; 374:179.
9. Najmoddina N, Ali B, Kavas H, Mohseni SM, Rezaie H, Johan Akerman Muhammet S, *et al.* XRD cation distribution and magnetic properties of mesoporous Zn-substituted $CuFe_2O_4$, Ceramics Internationl. 2014; 40:3619.
10. Amna Hassan, Muhammad Azhar Khan, Muhammad Shahid, Asghar M, *et al.* Muhammad Farooq Warsi., "Nanocrystalline $Zn_{1-x}Co_{0.5x}Ni_{0.5x}$ Fe_2O_4 ferrites: Fabrication via coprecipitation route with enhanced magnetic and electrical properties, Journal of Magnetism and Magnetic Materials. 2015; 393:56.
11. Rais A, Taibi K, Addou A, Zanoun A, Al-Douri Y. Copper substitution effect on the structural properties of nickel ferrites, Ceramics International. 2014; 40:14413.
12. Adel Maher Wahba, Mohamed Bakr Mohamed. Structural and magnetic characterization and cation distribution of nanocrystalline $Co_xFe_{3-x}O_4$ ferrites, Journal of Magnetism and Magnetic Materials. 2015; 378:246.
13. Zein K, Heiba, Mohamed Bakr Mohamed, DoganCation N. Cation distribution correlated with magnetic properties of nanocrystalline gadolinium substituted nickel ferrite, Journal of Magnetism and Magnetic Materials. 2015; 391:195.
14. Mohamed M, Wahba A, Yehia M. Structural and magnetic properties of $CoFe_{2-x}Mo_xO_4$nanocrystalline ferrites. Material science and Engineering. 2014; 190:52.
15. Maher Wahba A, Bakr Mohamed M. Structural, magnetic, and dielectric properties of nanocrystalline Cr-substituted $Co_{0.8}Ni_{0.2}Fe_2O_4$ ferrite. Ceramics international. 2014; 40:6127.
16. Bakr Mohamed M, Yehia M. Cation distribution and magnetic properties of Nanocrystalline gallium substituted cobalt ferrite, Journal of Alloys Compounds. 2014; 615:181.
17. Erum Pervaiz Gul IH. High frequency AC response, "DC resistivity and magnetic studies of holmium substituted Ni-ferrite: A novel electromagnetic material, Journal of Magnetism and Magnetic Materials. 2014; 349:27-34.
18. Hugh C, Neill, Alexandra Navrotsky. Simple spinels; crystallographic parameters, cation radii, lattice energies, and cation distribution, American Mineralogist. 1983; 68:181.
19. Ashour AH, Hemeda OM, Heiba ZK, Al-Zahrani SM. Electrical and thermal behavior of PS/ferrite composite, Journal of Magnetism and Magnetic Materials. 2014; 369:260.
20. Ghasemi A. ompositional dependence of magnetization reversal mechanism, magnetic interaction and Curie temperature of $Co_{1-x}Sr_xFe_2O_4$ spinel thin film. Journal of Alloys Compounds. 2015; 645:467-477.
21. Maaz K, Khalid W, Mumtaz A, Hasanain SK, Liu J, Duan JL. Magnetic characterization of $Co_{1-x}Ni_xFe_2O_4$ ($0 \leqslant x \leqslant 1$) nanoparticles prepared by co-precipitation route, Physica E. 2009; 41:593-599.